



# CHORUS

This is the accepted manuscript made available via CHORUS. The article has been published as:

## Fourier harmonics of high- $p_{\{T\}}$ particles probing the fluctuating initial condition geometries in heavy-ion collisions

Barbara Betz, Miklos Gyulassy, and Giorgio Torrieri

Phys. Rev. C **84**, 024913 — Published 25 August 2011

DOI: [10.1103/PhysRevC.84.024913](https://doi.org/10.1103/PhysRevC.84.024913)

# Fourier Harmonics of High- $p_T$ Particles Probing the Fluctuating Initial Condition Geometries in Heavy-Ion Collisions

Barbara Betz,<sup>1</sup> Miklos Gyulassy,<sup>1</sup> and Giorgio Torrieri<sup>2</sup>

<sup>1</sup>*Department of Physics, Columbia University, New York, 10027, USA*

<sup>2</sup>*Frankfurt Institute for Advanced Studies (FIAS), Frankfurt am Main, Germany*

Second Fourier harmonics of jet quenching have been thoroughly explored in the literature and shown to be sensitive to the underlying jet path-length dependence of energy loss and the differences between the mean eccentricity predicted by Glauber and CGC/KLN models of initial conditions. We compute the jet path-length dependence of energy-loss for higher azimuthal harmonics of jet-fragments in a generalized model of energy-loss for RHIC energies and find, however, that even the high- $p_T$  second moment is most sensitive to the poorly known early-time evolution during the first fm/c. Moreover, we demonstrate that higher-jet harmonics are remarkably insensitive to the initial conditions, while the different  $v_n(N_{part})$  vs.  $v_n^{JAA}(N_{part})$  correlations between the moments of monojet and dijet nuclear modification factors remain a most sensitive probe to differentiate between Glauber and CGC/KLN initial state sQGP geometries.

PACS numbers: 12.38.Mh,13.87.-a,24.85.+p,25.75.-q

## I. INTRODUCTION

Heavy-ion collisions at the Relativistic Heavy Ion Collider (RHIC) indicate the production of an opaque (i.e. strongly jet-suppressing) [1–5], strongly-coupled, fast-thermalizing medium that possibly needs to be described using methods derived from AdS/CFT string theory [6]. However, so far neither the initial conditions of the collisions nor the microscopic dynamics of the jet-energy loss are conclusively understood.

Two models are commonly used to characterize the initial conditions. The Glauber model [7], describing incoherent superpositions of proton-proton collisions, and the “Color Glass Condensate” (CGC) [8], given e.g. by the KLN model [9–11], where saturation effects are taken into account. They differ by their initial temperature gradients, their initial high- $p_T$  parton distribution, and the distance travelled by each parton, leading to a different opacity estimate. In addition, both models exhibit large event-by-event fluctuations [12–15].

The jet-energy loss can either be described as multiple scatterings of the parton [16–21], specific for a weakly-coupled pQCD medium, or using the AdS/CFT correspondence where the problem of a parton stopped in a thermal medium is related to the problem of a string falling into a 5-dimensional black hole [22–25].

Experimentally, jet-energy loss is parametrized by the suppression factor  $R_{AA}$ , defined as the ratio of jets produced in  $A+A$  collisions to the expectation for jets being produced in  $p+p$  collisions

$$R_{AA}(p_T) = \frac{dN^{A+A}/dp_T}{N_{coll}dN^{p+p}/dp_T}, \quad (1)$$

where  $N_{coll}$  is the number of collisions, a theoretical parameter (calculated within the Glauber model [13]) depending on centrality (i.e., on the number of participants  $N_{part}$ ).

The first attempt to disentangle the initial conditions (Glauber vs. CGC) and the energy-loss mechanism (pQCD vs. AdS/CFT) while simultaneously describing the nuclear modification factor  $R_{AA}(N_{part})$  and the elliptic flow  $v_2(N_{part})$  for high- $p_T$  particles was given in Refs. [26–28], favoring CGC initial conditions and a strongly-coupled energy loss at RHIC. A similar ansatz was used in Ref. [29], although the Fourier components were not shown explicitly.

To further study the differences of a pQCD and an AdS/CFT-like energy loss, we investigate the role of the energy dependence in the energy-loss prescription, examine the power of the path-length dependence, and calculate higher-jet harmonics. We want to examine if a generic energy-loss ansatz that includes both a path-length and an energy dependence confirms the above conclusion that only CGC initial conditions and an AdS/CFT energy-loss can describe both the  $R_{AA}(N_{part})$  and the  $v_2(N_{part})$  appropriately.

In the high-temperature limit, all dependences on the intrinsic scales of the system ( $T_c, \Lambda_{QCD}$ , etc.) disappear. Because of this, a generic energy-loss rate  $dE/dx$  is given by an arbitrary combination of dimensionful parameters constrained by the total dimension of the observable and the requirement that faster particles and hotter media result in a bigger suppression. We choose

$$\frac{dE}{dx}(\vec{x}_0, \phi, \tau) = -\kappa P^a \tau^z T^{z-a+2} [\vec{x}_0 + \hat{n}(\phi)\tau, \tau], \quad (2)$$

for an energy loss as a function of time  $\tau$  considering a jet starting at  $\vec{x}_0$  and propagating in direction  $\phi$  with the coupling  $\kappa$ .  $P$  is the momentum of the jet(s) considered,  $T$  is the temperature, and  $a, z$  are parameters controlling the jet energy (momentum) and path-length dependence, respectively.

In the Bethe-Heitler limit  $a = 1$  and  $z = 0$ , while in the deep LPM pQCD limit  $a \sim 0$  and  $z \sim 1$ . If  $a = 0$  and  $z = 2$ , our model coincides with the model referred to as “AdS/CFT” in Refs. [26, 28]. However, on-shell

AdS/CFT calculations [22–25] show that  $a = 1/3$  and  $z = 2$ , thus we are going to consider  $a = 1/3$  throughout the whole paper. However, one should keep in mind that  $a = 1/3$  is a weak lower bound for falling strings used for illustration. We note that, as it is clearly shown in Refs. [22–25],  $z = 2$  is only a *lower* limit corresponding to an “on-shell” quark whose stopping distance is  $l_f \gg 1/T$  and whose initial energy is  $E_0 \gg T$ . In a realistic medium, the first assumption is likely to be violated, resulting in values possibly of  $z > 2$ .

Please note that in contrast to Refs. [26–28],  $\kappa$  is a dimensionless parameter. In a particular case of radiative-dominated scattering in the LPM regime,  $\kappa T^3 \sim \hat{q}$  [30]. In general,  $\kappa$  measures the interaction cross-section, while  $T^3$  is related to the density of scattering centers. This (like soft observables in general) can be used as a constraint for  $\kappa$ , but additionally one has to assume nearly complete thermalization on the timescale of jet propagation throughout the system as well as a straight-forward relation between entropy density and multiplicity. While these assumptions are reasonable, they are not easily falsifiable, and, in particular, in the  $\hat{q}$ -limit, one finds that  $\kappa$  can *not* describe jet quenching and a realistic gluon density at the same time [30]. Therefore, we limit ourselves to fitting  $\kappa$  to the most central data point of  $R_{AA}$  measured at RHIC [27], disregarding any interpretation in terms of the density of soft degrees of freedom, comparing to the RHIC data on  $(\vec{x}_0, \phi)$ -averaged  $R_{AA}$  versus centrality for a range of  $E_f \sim 6 - 9$  GeV [27].

In a static medium,  $dE/dx \sim \tau^z$ , while in a dynamic medium,  $dE/dx$  will acquire additional powers of  $\tau$  due to the dependence of temperature on  $\tau$ , implicitly included in Eq. (2). Here, we assume a 1D Bjorken expansion [31]

$$T(\vec{x}, \tau) = T_0(\vec{x}) \left( \frac{\tau_0}{\tau} \right)^{1/3} \quad (3)$$

with different values of  $\tau_0$ . Surprisingly enough, we find that even the high- $p_T$  second Fourier moment ( $v_2$ ) is most sensitive to the poorly known early-time evolution during the first fm/c.

Considering that  $R_{AA}$  is given by the ratio of jets in the QGP to jets in vacuum, one obtains the following formula for the nuclear modification factor from Eq. (2) for a jet starting at  $\vec{x}_0$  and propagating in direction  $\phi$

$$R_{AA}(N_{part}, \vec{x}_0, \phi) = \exp[-\chi(\vec{x}_0, \phi)], \quad (4)$$

with

$$\chi(\vec{x}_0, \phi) = \left( \frac{1+a-n}{1-a} \right) \ln \left[ 1 - \frac{K}{P_0^{1-a}} I(\vec{x}_0, \phi, a, z) \right], \quad (5)$$

where  $n$  is the spectral index (taken to be  $n \sim 6$ ),  $K = \kappa(1-a)$ ,  $P_0$  is the jet’s initial momentum and the line integral is

$$I(\vec{x}_0, \phi, a, z) = \int_{\tau_0}^{\infty} \tau^z T^{z-a+2} [\vec{x}_0 + \hat{n}(\phi)\tau, \tau] d\tau. \quad (6)$$

In case of  $a = 1$  (the Bethe-Heitler limit),  $1/(1-a)$  diverges, but since  $K = \kappa(1-a) \rightarrow 0$ ,

$$\chi(\vec{x}_0, \phi) = \kappa(n-2)I(\vec{x}_0, \phi, a=1, z). \quad (7)$$

From the above calculated  $R_{AA}(N_{part}, \vec{x}_0, \phi)$ , the  $R_{AA}(N_{part})$  can be obtained by averaging over all possible  $\vec{x}_0$  and  $\phi$

$$\begin{aligned} R_{AA}(N_{part}) &= \int \frac{d\phi}{2\pi} \frac{\int R_{AA}(N_{part}, \vec{x}_0, \phi) T_{AA}(\vec{x}_0) d\vec{x}_0}{\int T_{AA}(\vec{x}_0) d\vec{x}_0} \\ &= \int \frac{d\phi}{2\pi} R_{AA}(N_{part}, \phi), \end{aligned} \quad (8)$$

where the nuclear overlap function is used in case of the Glauber model and  $T_{AA} = \rho^2/P_0^2$  for the CGC prescription.

After having fixed  $\kappa$ , the  $v_n(N_{part})$  can be computed via

$$v_n(N_{part}) = \frac{\int d\phi \cos\{n[\phi - \psi_n]\} R_{AA}(N_{part}, \phi)}{\int d\phi R_{AA}(N_{part}, \phi)}. \quad (9)$$

The Fourier density components  $e_n$  and the reaction-plane axis  $\psi_n$  are determined according to the initial density distribution used in Ref. [15]

$$e_n(t) = \frac{\sqrt{\langle r^2 \cos(n\phi) \rangle^2 + \langle r^2 \sin(n\phi) \rangle^2}}{\langle r^2 \rangle} \quad (10)$$

and

$$\psi_n(t) = \frac{1}{n} \tan^{-1} \frac{\langle r^2 \sin(n\phi) \rangle}{\langle r^2 \cos(n\phi) \rangle}. \quad (11)$$

By definition, the impact parameter points into the  $x$ -direction, but event-by-event fluctuations introduce non-trivial and harmonic dependent  $\psi_n$ ’s.

We checked that we reproduce the results of Ref. [26] when our approach is simplified to the one used in this reference, where

$$R_{AA}(N_{part}) = \langle e^{-\kappa I_m} \rangle, \quad (12)$$

and the line integral is

$$I_m = \int_0^{\infty} dl l^{m-1} \rho(\vec{r} + l\hat{v}), m = 1, 2, \dots \quad (13)$$

Here,  $m = 1$  and  $m = 2$  describe the path-length ( $l$ ) dependence for pQCD and AdS/CFT-like energy-loss, respectively. However, one of the main differences to our approach is that we also consider the energy dependence in the jet-energy loss. In other words,  $a = 0$  in Refs. [26–28] while we assume  $a = 1/3$  [see Eq. (2)] throughout the whole study.

The above analysis can be extended to dijets, analogously to Ref. [28]. Dijet suppression is parametrized by the factor  $I_{AA}$ , the ratio of the dijet suppression to the

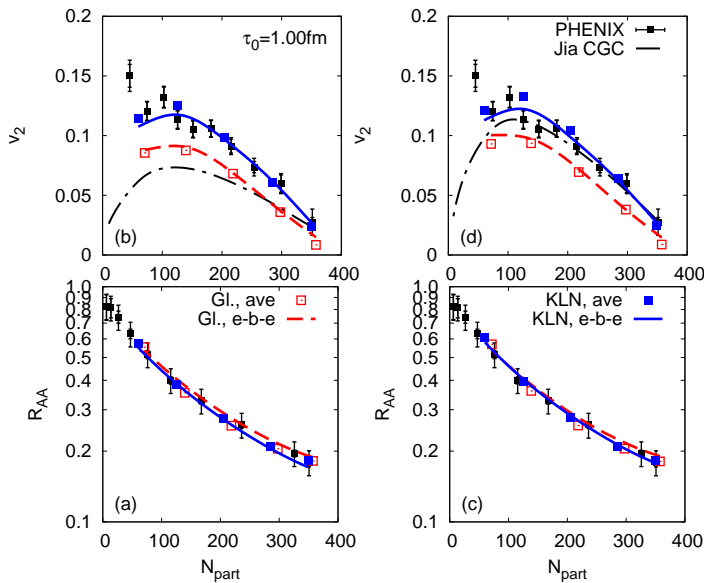


FIG. 1: (Color online)  $v_2$  (top panels) and  $R_{AA}$  (bottom panels) of high-momentum particles as a function of the number of participants,  $N_{part}$ , for  $z = 1$  (left panel) and  $z = 2$  [right panel, see Eq. (2) for definition] and  $\tau_0 = 1$  fm. The RHIC data are taken from Ref. [27].

suppression of jets, defined experimentally as in [32] and related to the parameters we defined earlier as in [28]

$$I_{AA} = \frac{dN_{dijet}^{A+A}/dp_T}{R_{AA}dN_{dijet}^{p+p}/dp_T} \simeq \frac{\langle e^{-\kappa(I^t + I^a)} \rangle}{R_{AA}}, \quad (14)$$

with the line integrals for the trigger (t) and away-side (a) jet. Please note that in contrast to Ref. [28], our coupling  $\kappa$  is equal for the trigger and the away-side jet. Clearly, a higher  $I_{AA}$  than  $R_{AA}$ , as observed in Ref. [32], implies that if one jet survives, the other one has a higher probability to survive as well. In turn, this indicates that jets emitted from less dense periphery regions have a larger impact. Thus, as remarked in Ref. [32], comparing jet abundance to dijet abundance can be a sensitive medium probe.

## II. RESULTS AND DISCUSSION

### A. Mean Correlations

We have carried out the procedure described in the previous section for a variety of impact parameters and initial conditions at RHIC energies. LHC energies have been mentioned in Ref. [33, 34] and will be explored in detail in Ref. [35]. In this subsection, we focus on the mean correlations. The width of these correlations will be discussed in the following subsection. Please note that this width is the actual physical geometry fluctuation.

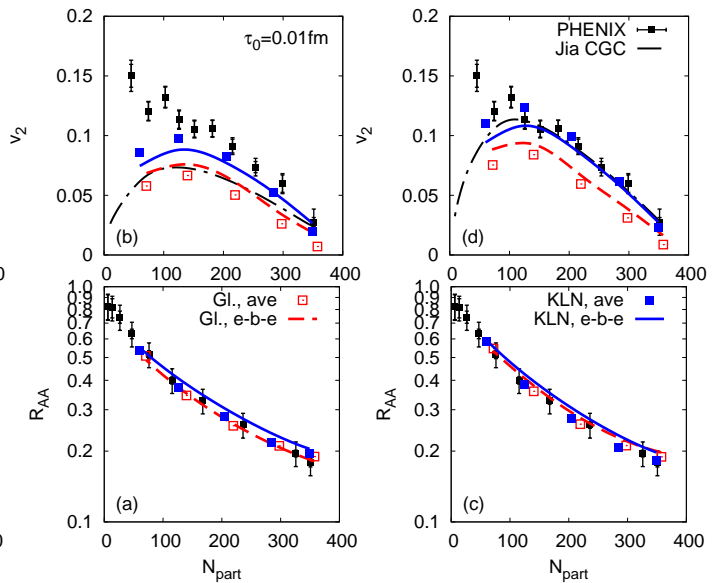


FIG. 2: (Color online)  $v_2$  (top panels) and  $R_{AA}$  (bottom panels) of high-momentum particles as in Fig. 1 for  $\tau_0 = 0.01$  fm.

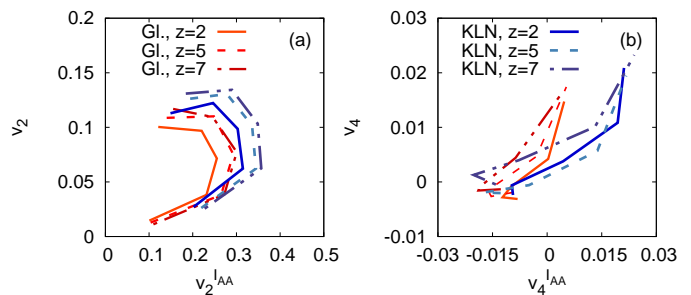


FIG. 3: (Color online) Higher Fourier coefficients of dijet observables,  $v_2^{IAA}$  vs.  $v_2$  (a) and  $v_4^{IAA}$  vs.  $v_4$  (b) for the Glauber model (reddish lines) and the KLN model (bluish lines) for  $z = 2, 5, 7$  and  $\tau_0 = 1$  fm. A clear shift between the Glauber and the KLN model as well as a saturation effect for larger  $z$  can be seen.

Throughout the paper, we distinguish four different cases. The Glauber model [7] and the CGC/KLN prescription [8–10], both event-by-event and averaged over many events, i.e. in the latter case the initial conditions are smoothed over many events and the energy loss is calculated subsequently.

In Fig. 1 we choose  $\tau_0 = 1$  fm, in line with recent hydrodynamic calculations [36]. The figure shows that for both Glauber (red) and KLN (blue) initial conditions as well as for both pQCD-like [Fig. 1 (a)] and AdS/CFT-like [Fig. 1(c)] energy loss the  $R_{AA}(N_{part})$  can be described choosing an appropriate value for  $\kappa$ . However, surprisingly enough, the results for  $v_2(N_{part})$  get close to the RHIC data when using KLN initial conditions for both pQCD-like [Fig. 1(b)] and AdS/CFT-like [Fig. 1(d)] energy loss, while Glauber initial conditions underpredict

the data. Moreover, the difference between pQCD-like and AdS/CFT-like energy loss is rather weak.

This result is a clear contradiction to the one shown in Ref. [27] and questions the conclusion that only CGC/KLN initial conditions and an AdS/CFT energy-loss can describe both the  $R_{AA}(N_{part})$  and the  $v_2(N_{part})$  appropriately. However, choosing a much smaller  $\tau_0$ , as done in Fig. 2, reduces the absolute value of  $v_2(N_{part})$  for both pQCD and AdS/CFT-like energy loss scenarios, while it increases the difference between the pQCD and AdS/CFT results as seen in Refs. [26, 27]. Here, the difference to the fit by Jia et al. [26] (black long dashed-dotted line), mainly seen for the pQCD-like energy-loss, is due to the additional energy loss dependence, parametrized by  $a = 1/3$ . Additionally, both plots show that there is a small discrepancy between the event-by-event and the averaged scenario [37].

We would like to mention here that in Refs. [26] different values of  $\tau_0$  were analyzed, nevertheless only the  $\tau_0 = 0$  fm case was shown in Ref. [27], leaving out a discussion about the physical meaning of  $\tau_0$ .

Setting  $\tau_0 = 1$  fm means to assume that there is no energy loss within the first fm. pQCD does not give any excuse for this assumption and thus  $\tau_0 = 0$  fm would be a natural assumption. However,  $\tau_0$  also describes the formation time of hydrodynamics which seems to be  $\tau_0 \sim 1$  fm [36]. On the other hand, setting  $\tau_0 = 1$  fm is also equivalent to the AdS/CFT result that the energy loss is suppressed at early times (due to the  $dE/dx \sim l^2$  dependence). Thus, it is important to note that the  $v_2$  of high- $p_T$  particles is sensitive to short-distance properties, suggesting that there is either weak coupling with a  $\tau_0 \sim 1$  fm or strong coupling which in itself features the suppression of energy loss at early times.

Extending the analysis to dijets and calculating the  $I_{AA}$ , our results meet the datapoint of Ref. [38] for both Glauber and KLN initial conditions when assuming that  $\kappa$  is the same for both parts of the dijet, in contrast to Ref. [28].

Since the energy loss calculated by AdS/CFT [22–25] clearly states that  $z = 2$  is only a lower limit, this raises the question which power in the jet path-length dependence has to be included when an AdS/CFT-like energy loss is considered. A detailed discussion of this issue will follow in the next subsection (see the Fig. 8).

Before that, we will focus on correlations of higher Fourier coefficients of dijet observables,  $v_2^{I_{AA}}$  vs.  $v_2$  and  $v_4^{I_{AA}}$  vs.  $v_4$ . Fig. 3 displays those correlations for the Glauber (reddish lines) and the KLN model (bluish lines) for  $z = 2, 5, 7$ .

A clear saturation effect occurs for larger  $z$  as well as a shift between the Glauber and the KLN model. Please note that while for the  $v_2$  correlation larger values of  $z$  of the Glauber model coincide with lower values of the KLN model, this is no longer true for the  $v_4$  correlations. Therefore, the different means of the correlations between  $v_n^{I_{AA}}(p_T)$  vs.  $v_n(p_T)$  remain a most sensitive probe to differentiate between CGC/KLN and Glauber initial state

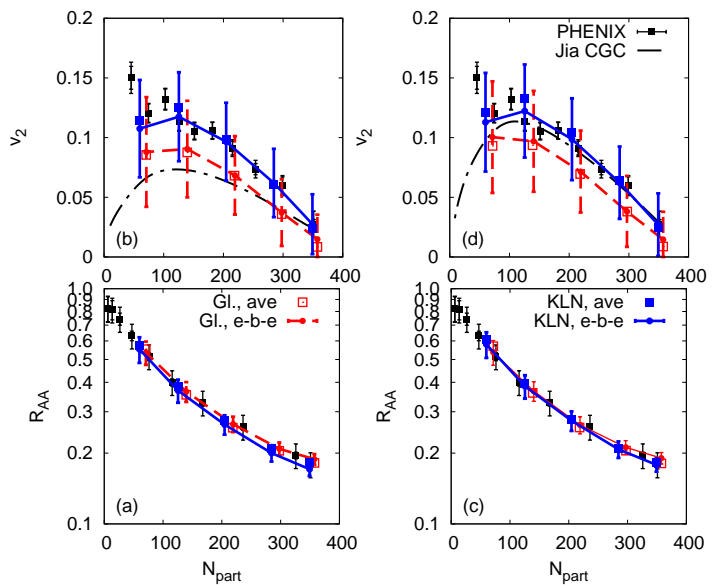


FIG. 4: (Color online) The fluctuation of  $v_2$  (top panels) and  $R_{AA}$  (bottom panels) of high-momentum particles as a function of the number of participants,  $N_{part}$ , for  $z = 1$  (left panel) and  $z = 2$  (right panel) and  $\tau_0 = 1$  fm. The RHIC data are taken from Ref. [27].

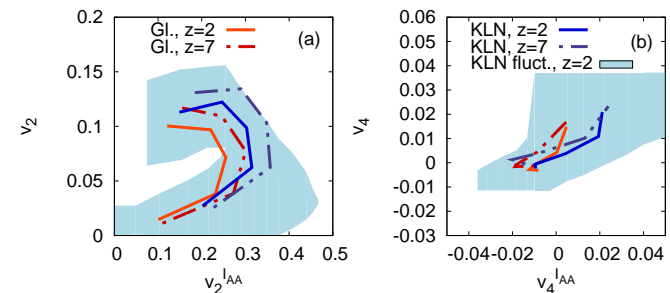


FIG. 5: (Color online) The fluctuation of the higher Fourier coefficients of dijet observables,  $v_2^{I_{AA}}$  vs.  $v_2$  (a) and  $v_4^{I_{AA}}$  vs.  $v_4$  (b) for the Glauber model (reddish lines) and the KLN model (bluish lines) for  $z = 2, 7$  and  $\tau_0 = 1$  fm. The blue area displays the region covered by the error bars of the KLN scenario for  $z = 2$ . The other cases show similar widths.

geometries.

## B. The Shallowness of the Correlations

After having focussed on the mean correlations in the last subsection, we now want to investigate the width of these correlations which is extremely important to conclude about the significance of the previously shown differences in the path-length dependence of the energy loss and the initial states considered.

Figs. 4 and 5 are a repetition of Figs. 1 and 3, including the fluctuations for the event-by-event analysis. As

can be seen, those fluctuations are small for  $R_{AA}(N_{part})$ , but the width for the  $v_2(N_{part})$  is rather large. Thus, in an experimental analysis it is less straightforward to distinguish between the different initial conditions than originally hoped for. Nevertheless, the CGC/KLN initial conditions seem to be favorable.

In Fig. 5 it becomes obvious that the while larger Fourier coefficients become smaller, their width becomes larger, making it experimentally more difficult to disentangle the different scenarios. Please note that the scale of Fig. 5(b) is larger than the one of Fig. 3(b), emphasizing the very broad event-by-event fluctuations of the higher-moment correlations. Therefore, in order to draw an experimentally testable conclusion, it is necessary to always determine the mean and the width of the correlations considered.

While the 2nd Fourier harmonics of jet quenching have been thoroughly investigated [26, 28, 39], the sensitivity of higher harmonics has remained relatively unexplored. In Ref. [29] higher harmonics were mentioned but not shown explicitly.

In a first step, we examine the differences in the eccentricities between the Glauber and the KLN model, see Figure 6. Here it becomes clear again that while on average differences certainly exist (that are bigger for  $e_2$  than for  $e_3$ ), the width of the distributions is again rather large. This is true both for harmonics present on average as well as event-by-event, such as  $e_2$ , and harmonics only present once fluctuations are taken into account, such as  $e_3$ , suggesting that higher harmonics of jet observables are rather insensitive to initial conditions.

Fig. 7 displays the mean and the width of  $v_3(N_{part})$  and  $v_4(N_{part})$  for Glauber and KLN initial conditions. While  $v_3$  is zero unless event-by-event fluctuations are taken into account,  $v_4$  is not too different between average and event-by-event initial conditions. Please note that the absolute amount of our  $v_3$  seems to be a little larger than reported but not shown in Ref. [29]. In both cases, however, even a hypothetical ideal experiment capable of determining the impact parameter precisely would be unable to distinguish between Glauber and CGC/KLN initial conditions using only jet harmonics, since event-by-event physical fluctuations are enough to draw out model sensitivity.

While higher-order coefficients are more sensitive to local gradients, they are also more susceptible to event-by-event fluctuations in initial conditions (hotspots, etc.), resulting in a larger  $v_{3,4}$  event-by-event fluctuation.

Fig. 8 shows the sensitivity of  $R_{AA}$  and  $v_n$  to the microscopic mechanism of energy loss, in particular to the power of the path-length dependence  $z$ . Here, we consider an impact parameter of  $b = 8$  fm that maximizes  $v_n$ . As can be seen, once  $R_{AA}$  is fixed via the coefficient  $\kappa$ , a residual sensitivity remains mostly in the Fourier components  $v_2$  and  $v_3$ . A saturation effect seems to occur for larger values of  $z$ .

Comparing the values of  $v_2$  obtained by the Glauber and the KLN model in Fig. 8 to the RHIC data obtained

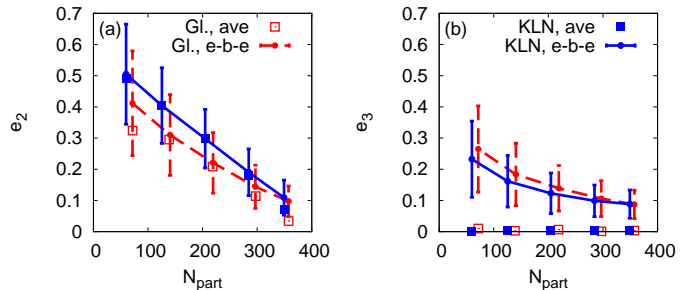


FIG. 6: (Color online) The eccentricity of the second (a) and third (b) Fourier components of the Glauber and KLN model, both event-by-event (red and blue lines) and averaged (red and blue dots). Since  $e_3$  is only present when fluctuations are taken into account, it has to vanish for the averaged analysis.

by the PHENIX experiment (black solid and dashed lines representing the datapoint at  $N_{part} = 125.7$  and its error-bar) [27] show that KLN initial conditions seem to favor lower and Glauber initial conditions higher exponents of the path-length dependence. Note that  $z > 2$  is allowed by AdS/CFT [22–25], combined with a significant parton virtuality (which is reasonable since the typical stopping length is *not*  $l_f \gg 1/T$ ). Since the virtuality can be directly measured in jet-photon collisions, the dependence of the exponent on virtuality could become a quantitative signature of AdS/CFT dynamics. Thus, a simultaneous measurement of  $v_2$ ,  $v_3$ , and  $v_4$  could elucidate the microscopic mechanism of jet-energy loss.

However, a question that naturally rises in this context is: Why are  $v_n$ 's at high- $p_T$  so insensitive to initial

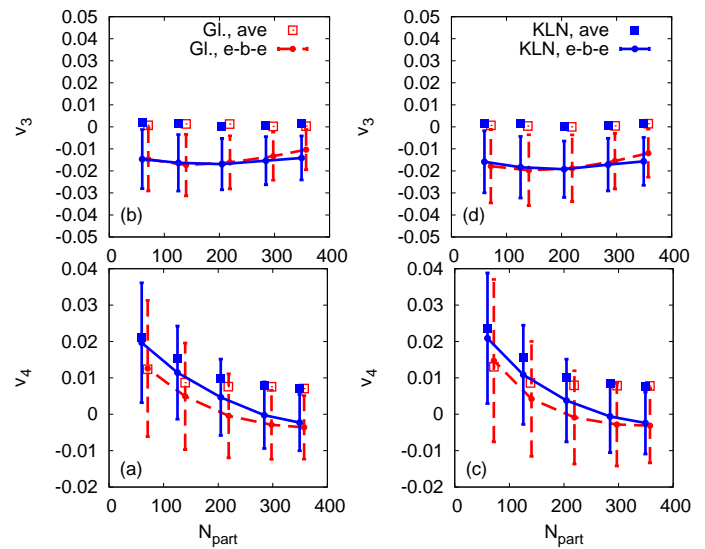


FIG. 7: (Color online)  $v_3$  (top panels) and  $v_4$  (bottom panels) of high-momentum particles as a function of the number of participants,  $N_{part}$ , for  $z = 1$  (left panel) and  $z = 2$  (right panel) and  $\tau_0 = 1$  fm.

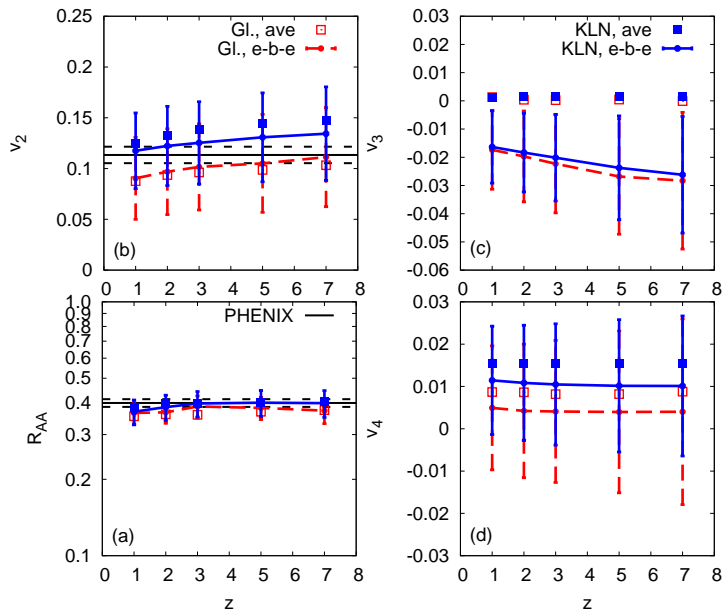


FIG. 8: (Color online)  $R_{AA}$  (a) and  $v_n$  (b-d) of high-momentum particles at an impact parameter of  $b = 8$  fm as a function of the path-length exponent  $z$ , defined in Eq. (2) for  $\tau_0 = 1$  fm. pQCD energy loss assumes that  $z = 1$  [26, 28, 39], for AdS/CFT on-shell partons  $z = 2$ , and AdS/CFT off-shell partons are  $z > 2$  [22–25]. A saturation effect can be seen for all  $v_n$  at large  $z$ . The RHIC data (black solid and dashed lines representing the datapoint at  $N_{part} = 125.7$  and its errorbar) are taken from Ref. [27].

conditions when hydrodynamics shows that the  $v_n$ 's of soft particles are extremely sensitive to initial conditions, leading to a systematic error of  $\mathcal{O}(100\%)$  in the viscosity [36]? In fact, the difference between these two regimes is *not* so surprising and can be readily understood physically. While viscous forces are driven by *local gradients* in flow, jet absorption is driven by *global differences* in the integrated  $\langle -\kappa P^a \tau^z T^{z-a+2} \rangle$ . The two effects are generally not the same and can indeed be very different if the distributions (like initial distributions of energy density in a Lorentz-contracted nucleus) are not smooth.

Both Glauber and KLN initial conditions are tuned

to reproduce the observed multiplicity distributions, and hence their  $\langle T \rangle$  is similar, even if the *local gradients* of  $T$  might be very different. Therefore, it follows that hydrodynamics and tomography lead to very different results.

In conclusion, we investigated different Fourier harmonics of jet quenching at RHIC energies and showed that the second Fourier coefficients [ $v_2(N_{part})$ ] are remarkably sensitive to the initial time  $\tau_0$ . If this  $\tau_0 = 1$  fm, as suggested by recent hydrodynamic calculations [36], then the conclusion drawn in Ref. [27] that only CGC/KLN initial conditions and an AdS/CFT-like energy loss can simultaneously describe the  $R_{AA}(N_{part})$  and  $v_2(N_{part})$  measured at RHIC can no longer be sustained. In contrast, for  $\tau_0 = 1$  fm both pQCD-like and AdS/CFT-like energy loss seem to reproduce the RHIC data well if CGC/KLN initial conditions are taken into account.

Moreover, we studied the microscopic mechanism of jet-energy loss by including an energy dependence and exploring the exponent  $z$  of the jet path-length dependence. We found that higher Fourier harmonics of jet quenching are remarkably insensitive to the differences between the Glauber and CGC/KLN model initial conditions. The different  $v_n^{IAA}(N_{part})$  vs.  $v_n(N_{part})$  correlations between the moments of monojet and dijet nuclear modifications factors remain a very sensitive probe to differentiate between Glauber and CGC/KLN initial conditions.

## Acknowledgments

B.B. is supported by the Alexander von Humboldt foundation via a Feodor Lynen fellowship. M.G. and B.B. acknowledge support from DOE under Grant No. DE-FG02-93ER40764. G.T. acknowledges the financial support received from the Helmholtz International Center for FAIR within the framework of the LOEWE program (Landesoffensive zur Entwicklung Wissenschaftlich-Ökonomischer Exzellenz) launched by the State of Hesse. The authors thank A. Dumitru for providing his KLN code to simulate the CGC initial conditions.

- 
- [1] M. Gyulassy and L. McLerran, Nucl. Phys. A **750**, 30 (2005); E. V. Shuryak, Nucl. Phys. A **750**, 64 (2005).
  - [2] I. Arsene *et al.* [BRAHMS Collaboration], Nucl. Phys. A **757**, 1 (2005).
  - [3] B. B. Back *et al.*, Nucl. Phys. A **757**, 28 (2005).
  - [4] J. Adams *et al.* [STAR Collaboration], Nucl. Phys. A **757**, 102 (2005).
  - [5] K. Adcox *et al.* [PHENIX Collaboration], Nucl. Phys. A **757**, 184 (2005).
  - [6] J. Noronha, M. Gyulassy and G. Torrieri, Phys. Rev. C **82**, 054903 (2010).
  - [7] M. L. Miller, K. Reygers, S. J. Sanders and P. Steinberg, Ann. Rev. Nucl. Part. Sci. **57**, 205 (2007).
  - [8] E. Iancu and R. Venugopalan, arXiv:hep-ph/0303204.
  - [9] D. Kharzeev and E. Levin, Phys. Lett. B **523**, 79 (2001).
  - [10] H. J. Drescher, A. Dumitru, C. Gombeaud and J. Y. Ollitrault, Phys. Rev. C **76**, 024905 (2007).
  - [11] H. J. Drescher, A. Dumitru, A. Hayashigaki and Y. Nara, Phys. Rev. C **74**, 044905 (2006).
  - [12] P. Sorensen, J. Phys. G **37**, 094011 (2010).
  - [13] B. Alver, M. Baker, C. Loizides and P. Steinberg, arXiv:0805.4411 [nucl-ex].
  - [14] R. Andrade, F. Grassi, Y. Hama, T. Kodama and O. J. Socolowski, Phys. Rev. Lett. **97**, 202302 (2006).

- [15] B. Alver and G. Roland, Phys. Rev. C **81**, 054905 (2010).
- [16] M. Gyulassy and X. n. Wang, Nucl. Phys. B **420**, 583 (1994).
- [17] M. Gyulassy, P. Levai and I. Vitev, Phys. Rev. Lett. **85**, 5535 (2000).
- [18] R. Baier, Y. L. Dokshitzer, A. H. Mueller, S. Peigne and D. Schiff, Nucl. Phys. B **484**, 265 (1997).
- [19] U. A. Wiedemann, Nucl. Phys. B **588**, 303 (2000).
- [20] J. w. Qiu and G. F. Sterman, Nucl. Phys. B **353**, 105 (1991).
- [21] P. B. Arnold, G. D. Moore and L. G. Yaffe, JHEP **0111**, 057 (2001).
- [22] S. S. Gubser, D. R. Gulotta, S. S. Pufu and F. D. Rocha, JHEP **0810**, 052 (2008).
- [23] P. M. Chesler, K. Jensen, A. Karch and L. G. Yaffe, Phys. Rev. D **79**, 125015 (2009).
- [24] P. M. Chesler, K. Jensen and A. Karch, Phys. Rev. D **79**, 025021 (2009).
- [25] P. Arnold and D. Vaman, arXiv:1101.2689 [hep-th].
- [26] A. Drees, H. Feng and J. Jia, Phys. Rev. C **71**, 034909 (2005); J. Jia and R. Wei, Phys. Rev. C **82**, 024902 (2010).
- [27] A. Adare *et al.* [PHENIX Collaboration], Phys. Rev. Lett. **105**, 142301 (2010).
- [28] J. Jia, W. A. Horowitz and J. Liao, arXiv:1101.0290 [nucl-th].
- [29] R. J. Fries and R. Rodriguez, Nucl. Phys. A **855**, 424 (2011).
- [30] J. Casalderrey-Solana and C. A. Salgado, Acta Phys. Polon. B **38**, 3731 (2007).
- [31] J. D. Bjorken, Phys. Rev. D **27**, 140 (1983).
- [32] A. Adare *et al.* [PHENIX Collaboration], Phys. Rev. C **78**, 014901 (2008).
- [33] W. A. Horowitz and M. Gyulassy, arXiv:1104.4958 [hep-ph].
- [34] B. Betz, M. Gyulassy and G. Torrieri, arXiv:1106.4564 [nucl-th].
- [35] B. Betz and M. Gyulassy, to be published.
- [36] H. Song, S. A. Bass, U. W. Heinz, T. Hirano and C. Shen, arXiv:1011.2783 [nucl-th].
- [37] T. Renk, H. Holopainen, J. Auvinen and K. J. Eskola, arXiv:1105.2647 [hep-ph].
- [38] A. Adare *et al.* [The PHENIX Collaboration], Phys. Rev. Lett. **104**, 252301 (2010).
- [39] C. Marquet and T. Renk, Phys. Lett. B **685**, 270 (2010).